

## Effect of Porous Substrate on the Strength of Asymmetric Structure

Chul Kim, Sang Hyun Park, Taewoo Kim, and Kee Sung Lee<sup>†</sup>

*School of Mechanical Systems Engineering, Kookmin University, Seoul 02707, Korea*

(Received August 11, 2015; Revised September 8, 2015; Accepted September 9, 2015)

### ABSTRACT

In this study, we investigate the effect of porous  $\text{Al}_2\text{O}_3$  substrate on the strengths of asymmetric structures after we prepare such a structure consisting of a dense  $\text{Li}_2\text{ZrO}_3$  top layer and porous  $\text{Al}_2\text{O}_3$  substrate layer. The porosity and elastic modulus of the substrate layer are controlled by sintering temperature, which has three values of 1150, 1250 and 1350°C. The porosity is controlled in the range of ~ 30-50 vol%, elastic modulus is ~80-120 GPa and elastic mismatch  $E_s/E_c$  is ~ 0.6-1.0. Indentation stress-strain curves are obtained and analyzed to evaluate the yield stress of the asymmetric structure by concentrated local loading of WC balls. Conventional flexural strengths are also obtained to evaluate the strength of the asymmetric structure. The results indicate that the local yield strength of the asymmetric structure has mid-values between the top and the substrate layer; however, the flexural strength of the asymmetric structure are mainly influenced by elastic modulus and strength of the substrate.

**Key words :** *Coatings, Porous materials, Strength, Elastic constants, Indentation*

### 1. Introduction

Asymmetric structure is generally defined for a layered structure with layers in non-symmetric characters. In a broader term, it often includes coated structures with layers in different thickness and laminated or sandwiched structure with layers of different properties, although the thickness is similar.<sup>1-3)</sup> The terminology, asymmetric structure, has been frequently used for porous membranes<sup>2)</sup> and fuel cells.<sup>1)</sup> In these cases, the introduced porosity can provide light-weight and consequent energy saving to the systems. An additional functionality can be realized if one of the layers is a functionally active layer or coating.

Figure 1 is a schematic diagram of asymmetric structures with (a) bi-layer and (b) tri-layer. A variety of ceramics belong to this category; for example, energy ceramics such as insulating refractory ceramics,<sup>4)</sup> super light-weight and high-strength engineering ceramics,<sup>5,6)</sup> membranes, fuel cells and coating materials for gas turbine.<sup>7,8)</sup> Functionally-gradient bioceramics<sup>9)</sup> and multilayered electromagnetic ceramics<sup>10)</sup> also belong to the asymmetric structure.

Porous ceramics have been developed for filters, membranes, fuel cells and engineering ceramics. When pores are introduced into ceramics, the net area for load bearing decreases, and mechanical strength is thus reduced exponentially. However, whenever flow of fluids through the body or a reduced body weight is required, pores could pro-

vide the roles. This has stimulated a continuous research on the subject.<sup>11,12)</sup> Some studies reported very promising results that reduction of strength could be minimized by controlling size, size distribution, and shape of pores.<sup>13,14)</sup> Another report claimed that a proper control of pore distribution can enhance resistance to mechanical damages.<sup>15)</sup>

When a light-weight asymmetric structure is used as a component, the energy is saved in any energy or mechanical systems. The component is normally interconnected with other components, and thus often operates under a constrained condition via the component-to-component contact. Even if there is no direct contact, contact with fluids is quite common for the component, and maintaining mechanical strength under this condition is a prime concern to prolong the component's lifetime. Considering the strain is constant under this condition, its elastic modulus is especially critical, since a difference in elastic modulus leads to stress development by the Hook's law, and excessive stress could result in fracture of the component.<sup>16-18)</sup>

In this study, we prepared  $\text{Li}_2\text{ZrO}_3$ <sup>19,20)</sup> membrane that can selectively separate carbon dioxide at high temperatures. We adopted a porous alumina ( $\text{Al}_2\text{O}_3$ ) as the substrate to make the component lighter and to have easy flow of gases through it. We sintered the substrates at different temperatures to vary their porosities. By bonding the membrane on the prepared substrates, we fabricated the bonded asymmetric structures with different elastic moduli and with the corresponding elastic mismatches.<sup>15)</sup> With these prepared specimens under the arranged constrain, we aim to evaluate the effect of porous substrate on properties of the whole asymmetric component by employing SEM, indentation method,<sup>21)</sup> and flexural strength test.

<sup>†</sup>Corresponding author : Kee Sung Lee

E-mail : keeslee@kookmin.ac.kr

Tel : +82-2-910-4834 Fax : +82-2-910-4839

## 2. Experimental Procedure

For the fabrication of  $\text{Li}_2\text{ZrO}_3$  top layer,  $\text{Li}_2\text{CO}_3$  (Aldrich, USA) and 8 mol% YSZ (Tosoh, Japan) powders at 1:1 mole ratio were wet milled with isopropyl alcohol and zirconia balls for 24 h. The milled slurry was calcined in an alumina crucible at temperatures of 800~ 900°C to synthesize  $\text{Li}_2\text{ZrO}_3$  powder. We dispersed the synthesize powder in solvent made of toluene (Kanto, Japan) and 2-propanol (Kanto, Japan) at volume ratio of 5 : 1 with 1 wt% of dispersion agent (Fish Oil, Sigma, USA) for 24 h. We finally prepared  $\text{Li}_2\text{ZrO}_3$  slurry by further wet ball milling for 24 h with the addition of PVB (Poly Vinyl Butyral, Aldrich, USA) and DBP (Dibutyl Phthalate, Aldrich, USA) as binder and plasticizer, respectively.

The prepared slurry was de-aired in a vacuum and formed to  $\text{Li}_2\text{ZrO}_3$  tape on a tape caster (Hansung system Inc., Korea). We fabricated  $\text{Li}_2\text{ZrO}_3$  laminate (~ 6 mm thick) by stacking ten  $\text{Li}_2\text{ZrO}_3$  tapes ( $30 \times 30$  mm) with lamination machine (Hansung system Inc., Korea) at 80°C under uniaxial pressure of 400 kgf/cm<sup>2</sup> for 10 min. The laminate was heat treated at a heating rate of 0.5°C/min at 600~800°C to remove organic substances, and sintered at 1600°C to have relative density higher than 90%.

For the fabrication of porous alumina ( $\text{Al}_2\text{O}_3$ ) substrates, we ball milled in a wet condition by mixing alumina powder (0.4  $\mu\text{m}$ , Alcoa, Japan) with the addition of 3 wt% PVB as the binder. The milled slurry was dried, crushed, and sieved to powders. We then prepared the substrates with controlled porosities by forming the powder in a mold at pressure of 200 kgf/cm<sup>2</sup>, and sintering at 1150°C, 1250°C, 1350°C, and 1400°C, which gave a porosity range of 30 ~ 50%.

We fabricated asymmetric structures by bonding the  $\text{Li}_2\text{ZrO}_3$  laminate ( $0.5 \times 4 \times 20$  mm) on the sintered alumina substrates ( $3 \times 4 \times 30$  mm) with epoxy.<sup>15,17</sup> Before the bonding, both surfaces of  $\text{Li}_2\text{ZrO}_3$  tape were polished with SiC abrasive powder (600 grit) to create microcracks in order to evaluate their effect on the strength of asymmetric structures.

Elastic modulus of sintered alumina in terms of porosity was estimated by the following Kundsens equation:<sup>22)</sup>

$$E = E_0 \exp(-bp) \quad (1)$$

Here,  $E_0$  is set to 370 GPa which corresponds to the elastic modulus of alumina with relative density higher than 99%, and  $b$ , an empirical constant 3.44, considering sintering conditions.<sup>23)</sup>

We analyzed microstructure of fractured surfaces of alumina substrates by SEM. We also measured strength of asymmetric structures ( $3 \times 4 \times 30$  mm) by the 3-point MOR (modulus of rupture) method. The loading setup was so arranged that the surface of  $\text{Li}_2\text{ZrO}_3$  layer was under tensional stress with span of 20.15 mm and loading speed of 0.2 mm/min. Specimen surfaces were polished with SiC abrasive paper (#2000), and their edges were properly chamfered.

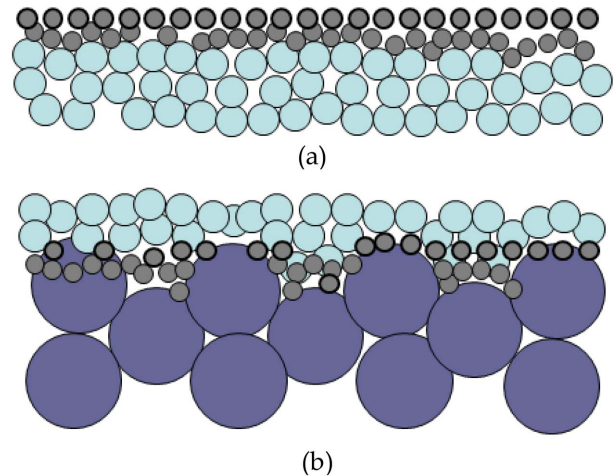


**Fig. 1.** Schematic diagram of asymmetric structures with (a) bi-layer and (b) tri-layer.

For indentation test, the  $\text{Li}_2\text{ZrO}_3$  tape and alumina substrates fired at 1150, 1250, and 1350°C were prepared in thickness of 4 mm each. In addition, their bonded specimens of asymmetric structures were also prepared. All surfaces for indentation test were polished with 1  $\mu\text{m}$  diamond suspension to mirror surface. By using a universal testing machine (Instron 5567, U.S.A.), a range of loads ( $P$ ) from 5 N to maximum 1500 N were applied on the surface of each specimen with a WC ball indenter (radius = 3.18 mm). At each  $P$ , diameter ( $a$ ) of the generated indent was measured by an optical microscope, and indentation stress  $p_0$  and indentation strain<sup>24)</sup> were calculated by the following equations:

$$\text{Indentation stress, } p_0 = P/\pi a^2 \quad (2)$$

$$\text{Indentation strain, } a/r \quad (3)$$

## 3. Results and Discussion

Figure 2 shows porosity of alumina substrate in terms of sintering temperature, which demonstrates reduced apparent porosity with increasing sintering temperature. Specimen fired at 1400°C, which is the highest temperature employed in this study, has an apparent porosity of 26.2%, while the specimen fired at 1350°C has 32.2%. According to percolation theory, pores cannot be interconnected when porosity falls down below 30%,<sup>25)</sup> and the resulted closed pores will make the flow of gases through the system very difficult. Therefore, the substrate fired at 1400°C was removed from evaluation, and the substrates fired at 1150°C, 1250°C, and 1350°C, and having a porosity range of 32.2 ~ 49% were evaluated and used as the substrate for fabrication of the asymmetric structure.

As shown in Fig. 3, porosity data from Fig. 2 were substituted into Equation (1), and elastic moduli of alumina substrates sintered at 1150°C, 1250°C, and 1350°C were calculated as 77 GPa, 91.9 GPa, and 121.9 GPa, respec-

tively. It clearly reveals that higher sintering temperature reduced porosity and increased elastic modulus.

In this study, we bonded two prepared layers by epoxy instead of by sinter-bonding to model and characterize the system under constrained condition with applied flexural stress. The thickness of epoxy bonding was kept under  $10\ \mu\text{m}$ , since previous studies claimed that the effect of epoxy on

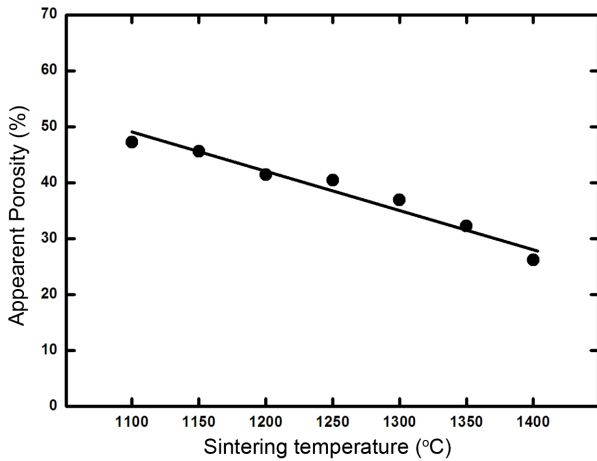


Fig. 2. Apparent porosities of the porous  $\text{Al}_2\text{O}_3$  substrates sintered at different temperatures.

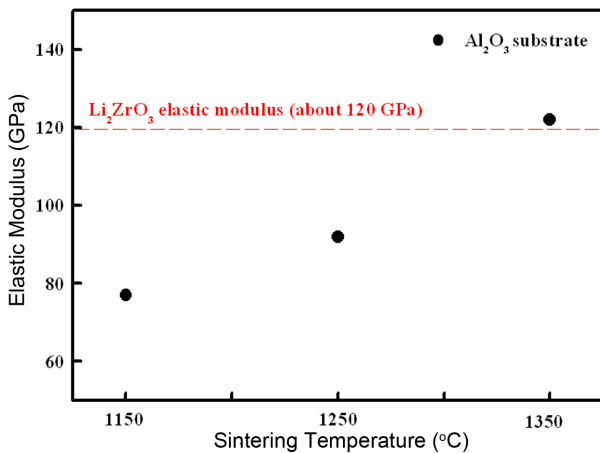


Fig. 3. Elastic moduli of the  $\text{Li}_2\text{ZrO}_3$  layer and the porous  $\text{Al}_2\text{O}_3$  layers fabricated at different sintering temperatures.

property of the system is negligible as long as the thickness of the bonding is under  $10\ \mu\text{m}$ .<sup>21)</sup>

The generated elastic mismatch between the  $\text{Al}_2\text{O}_3$  substrate layer and top  $\text{Li}_2\text{ZrO}_3$  layer is defined by elastic modulus of former ( $E_s$ ) divided by that of the later ( $E_c$ ), and Fig. 4 shows the result based on elastic moduli calculated in Fig. 3. As indicated in the graph, elastic modulus of 121.9 GPa for the substrate fired at  $1350^\circ\text{C}$  is almost same as that of  $\text{Li}_2\text{ZrO}_3$ , implying that the difference in elastic modulus would not cause any effect under external force. Therefore, the optimal asymmetric structure can be designed to cause no resistance to gas permeation, to have relatively high mechanical property, and to have the minimal elastic mismatch between the coating and the alumina substrate fired at  $1350^\circ\text{C}$ .

Figure 5 shows microstructural images for fractured surface of alumina substrates fired at 1150, 1250, and  $1350^\circ\text{C}$ . The images indicate that increase in sintering temperature decreases porosity, which led to a denser body with more grain growth. As analyzed in the previous studies on density and microstructure of  $\text{Li}_2\text{ZrO}_3$ ,<sup>19)</sup> we confirmed that the substrates are quite dense with densities in the range of  $4.0 \sim 5.0\ \text{g}/\text{cm}^3$ , which corresponds to the same or higher than theoretical density of  $4.418\ \text{g}/\text{cm}^3$ .

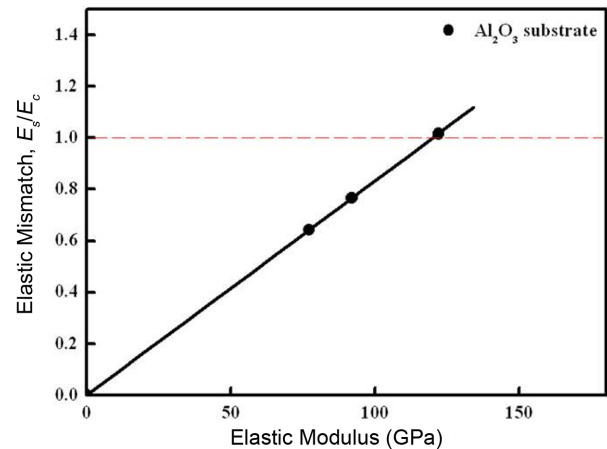


Fig. 4. Elastic mismatches between the  $\text{Li}_2\text{ZrO}_3$  layer and the porous  $\text{Al}_2\text{O}_3$  substrates fabricated at different sintering temperatures. The mismatch is plotted as a function of elastic modulus of the porous  $\text{Al}_2\text{O}_3$  substrate.

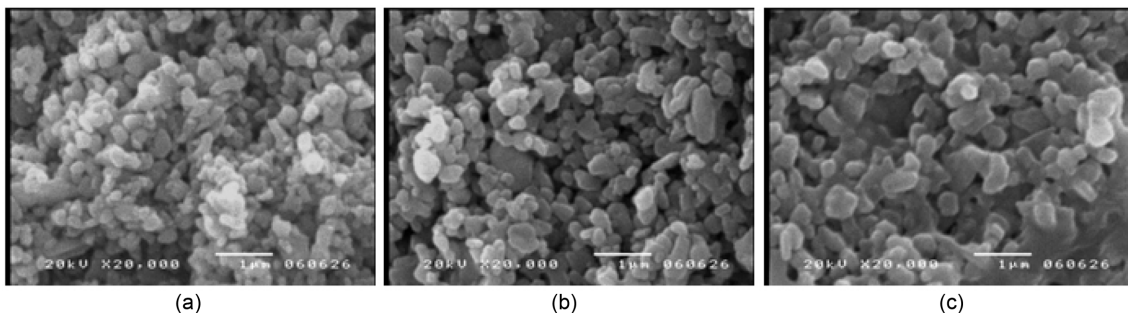
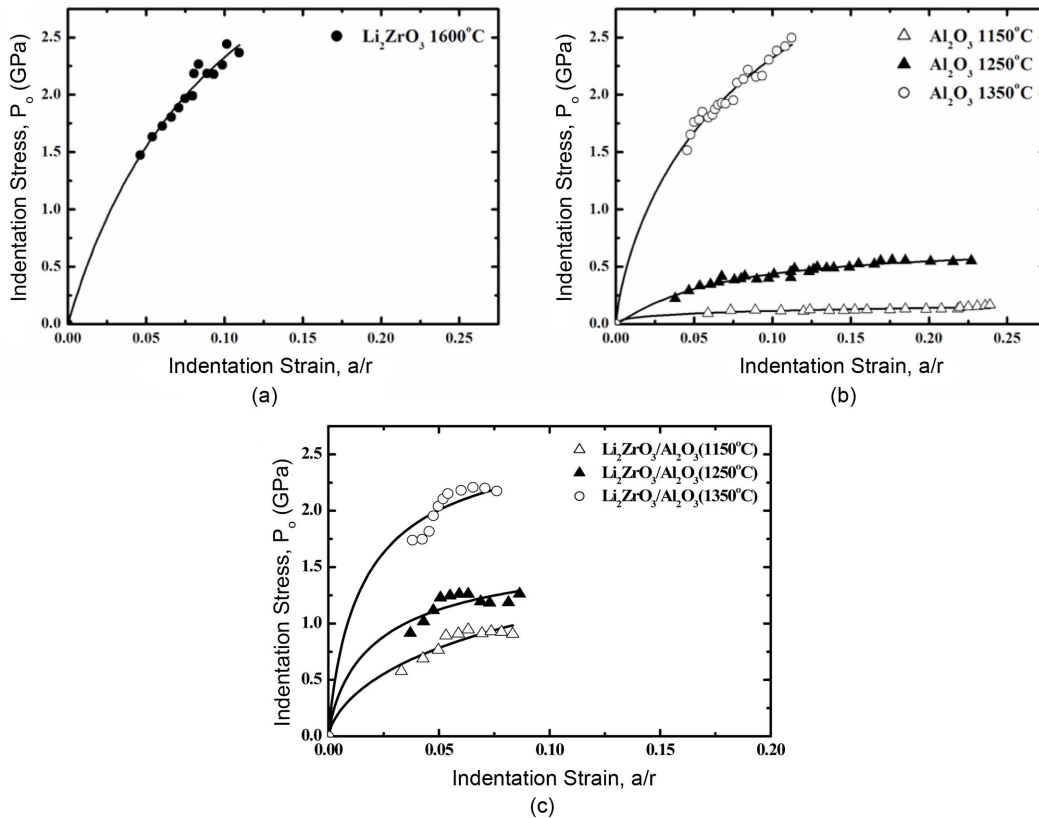


Fig. 5. SEM micrographs of the porous  $\text{Al}_2\text{O}_3$  substrates fabricated at uniaxial pressing of  $200\ \text{kgf}/\text{cm}^2$  and sintering at (a)  $1150^\circ\text{C}$ , (b)  $1250^\circ\text{C}$ , and (c)  $1350^\circ\text{C}$ .



**Fig. 6.** Indentation stress-strain curves from the spherical indentation method for (a) the  $\text{Li}_2\text{ZrO}_3$  layer, (b) the porous  $\text{Al}_2\text{O}_3$  substrates sintered at 1150, 1250 and 1350°C, and (c) the  $\text{Li}_2\text{ZrO}_3/\text{porous Al}_2\text{O}_3$  asymmetric structures.

Figure 6(a) shows indentation stress-strain curve obtained from indentation with WC ball indenter on dense  $\text{Li}_2\text{ZrO}_3$  bodies, giving a high yield stress of 1.0 ~ 1.5 GPa. Fig. 6(b) is the indentation results for the alumina substrates sintered at 1150°C, 1250°C, and 1350°C. The one sintered at 1350°C shows relatively lower porosity and gives yield stress as high as that of  $\text{Li}_2\text{ZrO}_3$ , while a further increase in porosity results in drastic decrease in yield stress. Fig. 6(c) is the indentation results with the asymmetric structures fabricated by bonding the  $\text{Li}_2\text{ZrO}_3$  layer of Fig. 6(a) and the substrates of Fig. 6(b). Their yield stress data with the alumina substrates sintered at 1150°C and 1250°C are increased due to the effect by  $\text{Li}_2\text{ZrO}_3$ . On the other hand, that of asymmetric structure with the alumina substrate sintered at 1350°C is the highest, and similar to those of  $\text{Li}_2\text{ZrO}_3$  and monolith substrate.

Figure 7 shows results by 3-point MOR for asymmetric structures with microcracks on top surface of the  $\text{Li}_2\text{ZrO}_3$  layer when the top surface was under tensional stress. The measured 3-point MOR were 15 MPa, 36.9 MPa, and 71.8 MPa for the three cases of different substrates, respectively. When microcracks were introduced on both surfaces of the  $\text{Li}_2\text{ZrO}_3$  layer, the values were 14.2 MPa, 39.5 MPa, and 72.6 MPa for each case. For the  $\text{Li}_2\text{ZrO}_3$  layer alone, it was 45.7 MPa, while alumina substrates alone were 11.1 MPa, 31.2 MPa, and 81.6 MPa for the three cases. The results

clearly indicate that when strength of substrate layer is higher than that of coating layer, the strength of layered system increases. However, the effect of introduced microcracks on one or both sides of the  $\text{Li}_2\text{ZrO}_3$  layer is not clearly defined. Based on these results, we confirmed that the porous substrate critically affects the strength of the overall structure, and concluded that asymmetric structure of lightweight and enhanced strength can be fabricated by bonding

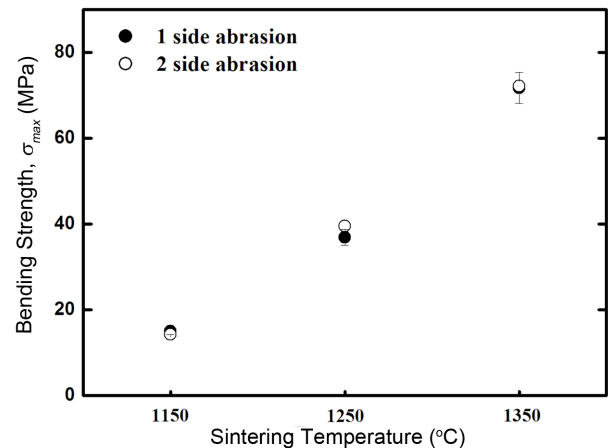


**Fig. 7.** Flexural strength data of the  $\text{Li}_2\text{ZrO}_3/\text{porous Al}_2\text{O}_3$  asymmetric structures.

a dense  $\text{Li}_2\text{ZrO}_3$  on an alumina substrate with porosity of about 30% by controlled sintering at 1350°C.

#### 4. Conclusions

In this study, we prepared a dense  $\text{Li}_2\text{ZrO}_3$  membrane and porous alumina substrates with ranges of different porosities (30 ~ 50%) and elastic moduli (77~121.9 GPa) by sintering at different temperatures. By bonding the membrane on the prepared substrates, we fabricated asymmetric structures under the preset constrain. We evaluated the effect of porous substrate on properties of the whole asymmetric component by indentation method and flexural strength test.

The results show that strength of the system decreases if strength of the substrate layer is lower than that of the coating layer or the difference of elastic modulus between the two layers is bigger than a certain number. We conclude that the porous substrate critically affects on strength of the bi-layer structure. The system strength is not much influenced by the presence of microcracks on surface or interface of the  $\text{Li}_2\text{ZrO}_3$  membrane, which supports the conclusion that the substrate layer is critical.

We demonstrate an optimal design for an asymmetric structure of light-weight and enhanced strength by bonding a dense  $\text{Li}_2\text{ZrO}_3$  membrane on an alumina substrate with porosity of about 30% by controlled sintering at 1350°C. The so-prepared substrate can provide an easy excess for gases due to its higher porosity, a better mechanical strength to the system due to its higher strength than that of the membrane, and a minimal elastic modulus mismatch between two layers due to its similar elasticity to that of the counterpart. This will eventually lead to a better durability and a prolonged lifetime for the component.

#### Acknowledgments

This work was conducted by research program 2014 Kookmin University.

#### REFERENCES

1. S. Lee, K. S. Lee, S. K. Woo, J. W. Kim, T. Ishihara, and D. K. Kim, "Oxygen-Permeating Property of  $\text{LaSrBFeO}_3$  (B=Co, Ga) Perovskite Membrane Surface-Modified by  $\text{LaSrCoO}_3$ ," *Solid State Ionics*, **158** 287-96 (2003).
2. X. Tan, Y. Liu, and K. Li, "Mixed Conducting Ceramic Hollow-Fiber Membranes for Air Separation," *AIChE Journal*, **51** [7] 1991-2000 (2005).
3. J. H. Park, E. Lee, T. W. Kim, H. J. Yim, and K. S. Lee, "Fracture Behavior of Glass/Resin/Glass Sandwich Structures with Different Resin Thicknesses," *Trans. Korean Soc. Mech. Eng. A*, **34** [12] 1849-56 (2010).
4. G. H. Cho, E. H. Kim, Y. G. Jung, and Y. K. Byeun, "Improving Oxidation Resistance and Fracture Strength of MgO-C Refractory Material Through Precursor Coating," *Surf. Coat. Technol.*, **260** 429-32 (2014).
5. K. S. Lee, S. K. Lee, B. R. Lawn, and D. K. Kim, "Contact Damage and Strength Degradation in Brittle/Quasi-Plastic Silicon Nitride Bilayers," *J. Am. Ceram. Soc.*, **81** [9] 2394-404 (1998).
6. J. B. Davis, A. Kristoffersson, E. Carlström, and W. J. Clegg, "Fabrication and Crack Deflection in Ceramic Laminates with Porous Interlayers," *J. Am. Ceram. Soc.*, **83** [10] 2369-74 (2000).
7. K. S. Lee, K. I. Jung, Y. S. Heo, T. W. Kim, Y. G. Jung, and U. Paik, "Thermal and Mechanical Properties of Sintered Bodies and EB-PVD Layers of  $\text{Y}_2\text{O}_3$  Added  $\text{Gd}_2\text{Zr}_2\text{O}_7$  Ceramics for Thermal Barrier Coatings," *J. Alloys Compd.*, **507** 448-55 (2010).
8. K. S. Lee, D. H. Lee, and T. W. Kim, "Microstructure Controls in Gadolinium Zirconate/YSZ Double Layers and Their Properties," *J. Ceram. Soc. Jpn.*, **122** [8] 668-73 (2014).
9. Y. H. Hsu, I. G. Turner, and A. W. Miles, "Fabrication of Porous Bioceramics with Porosity Gradients Similar to the Bimodal Structure of Cortical and Cancellous Bone," *J. Mater. Sci.*, **18** 2251-56 (2007).
10. J. H. Kang, H. M. Cha, Y. G. Jung, and U. Paik, "Crack Suppression and Residual Stress in  $\text{BaTiO}_3$  Based Ni-MLCCs of Y5V Specification through Post-Process," *J. Mater. Process. Technol.*, **205** 160-67 (2008).
11. K. S. Lee, S. K. Woo, I. S. Han, D. W. Seo, S. J. Park, and Y. O. Park, "Filtering Characteristics of Porous SiC Filter with High Surface Area," *J. Ceram. Soc. Jpn.*, **110** [7] 656-61 (2002).
12. Y. Zhang, F. He, S. Xia, L. Kong, D. Xu, and Z. Wu, "Adsorption of Sediment Phosphorus by Porous Ceramic Filter Media Coated with Nano-Titanium Dioxide Film," *Ecol. Eng.*, **64** 186-92 (2014).
13. K. S. Lee, D. W. Seo, J. H. Yu, and S. K. Woo, "A Study on the Improvement of Strength in NiO-YSZ Porous Anode Material for Solid Oxide Fuel Cell," *J. Korean Ceram. Soc.*, **40** [3] 241-48 (2003).
14. G. Pia, L. Casnedi, M. Ionta, and U. Sanna, "On the Elastic Deformation Properties of Porous Ceramic Materials Obtained by Pore-Forming Agent Method," *Ceram. Int.*, **41** 11097-105 (2015).
15. K. S. Lee, S. K. Kim, C. Kim, T. W. Kim, and D. K. Kim, "Cracking of Densely Coated Layer Adhesively Bonded to Porous Substrates Under Hertzian Stress," *J. Mater. Sci.*, **42** 9116-20 (2007).
16. K. S. Lee, S. Wuttiaphan, X. Z. Hu, S. K. Lee, and B. R. Lawn, "Contact-Induced Transverse Fractures in Brittle Layers on Soft Substrates: A Study on Silicon Nitride Bilayers," *J. Am. Ceram. Soc.*, **81** [3] 571-80 (1998).
17. K. S. Lee, Y. W. Rhee, D. H. Blackburn, and B. R. Lawn, "Cracking of Brittle Coatings Adhesively Bonded to Substrates of Unlike Modulus," *J. Mater. Res.*, **15** [8] 1653-56 (2000).
18. K. S. Lee, K. S. Jang, J. H. Park, T. W. Kim, I. S. Han, and S. K. Woo, "Designing the Fiber Volume Ratio in SiC Fiber-Reinforced SiC Ceramic Composites," *Mater. Des.*, **32** 4394-401 (2011).
19. S. H. Park, S. Lee, J. H. Yu, S. K. Woo, and K. S. Lee, "Fabrication of  $\text{Li}_2\text{ZrO}_3$  Membrane and Evaluation on the

- Mechanical Properties Before and After CO<sub>2</sub> Separation," *J. Korean Ceram. Soc.*, **44** [1] 58-64 (2007).
20. B. N. Nair, R. P. Burwood, V. J. Goh, K. Nakagawa, and T. Yamaguchi, "Lithium Based Ceramic Materials and Membranes for High Temperature CO<sub>2</sub> Separation," *Prog. Mater. Sci.*, **54** 511-41 (2009).
21. B. R. Lawn, "Indentation of Ceramics with Spheres: A Century after Hertz," *J. Am. Ceram. Soc.*, **81** [8] 1977-94 (1998).
22. J. H. Ha, J. H. Kim, and D. K. Kim, "Elasticity and Thermal Conductivity of Porous Ceramics with Controlled Pore Structure," *J. Ceram. Soc. Jpn.*, **112** [5] 1084-88 (2004).
23. R. W. Rice, "Comparison of Stress Concentration Versus Minimum Solid Area Based Mechanical Property-Porosity Relation," *J. Mater. Sci.*, **28** 2187-90 (1993).
24. D. H. Lee and K. S. Lee, "Mechanical Behavior of Layered YSZ Thermal Barrier Coatings using Indentation Test," *J. Korean Ceram. Soc.*, **48** [5] 396-403 (2011).
25. A. Davison and M. Tinkham, "Phenomenological Equations for the Electrical Conductivity of Microscopically Inhomogeneous Materials," *Phys. Rev.*, **13** [8] 3261-67 (1976).